A FLEXIBLE DIGITAL RECEIVER ARCHITECTURE FOR SPACE DEBRIS MEASUREMENTS, ASTRONOMY AND SPACE RECONNAISSANCE

G. Bartsch[1] and B. Klein[2]

[1] FGAN - Research Institute for High Frequency Physics and Radar Techniques (FHR), Neuenahrer Strasse 20, D-53343 Wachtberg-Werthhoven, Germany; Bartsch@FGAN.de

[2] Max-Planck-Institut für Radioastronomie (MPIfR), Auf dem Hügel 69, D-53121 Bonn, Germany; BKlein@MPIfR-Bonn.mpg.de

ABSTRACT

Beam-park experiments done by powerful and highly sensitive radar allow us to gain insight into the debris population. But any cost-effective approach demands a multi-use concept where the system can be reconfigured easily to perform a variety of different tasks. In this paper we present a flexible digital receiver architecture for space debris measurements which supports many other fields of space research.

Key words: digital receiver; space debris; radio astronomy; space reconnaissance.

1. INTRODUCTION

Near-earth space is occupied by numerous man-made objects, both operational satellites and space debris. Moreover, the number of these objects is steadily increasing despite the cleansing effect of the atmospheric drag. Objects with a size greater than 10 cm are cataloged by the U.S. Strategic Command (USSTRATCOM) Space Surveillance Network (SSN). For those objects one has a survey of the space debris situation and is able to validate models like ESA's MASTER (Meteoroids and Space Debris Terrestrial Reference) model.

To inspect the debris population and to validate the model even for objects down to the sub-centimeter sized regime, one has to measure this fine-scale part of the population.

Within the scope of the ESA-funded beam-park experiment COBEAM in 1996 it was demonstrated that Europe has a system which is able to detect debris down to a minimum size of 9 mm at 1000 km slant range. For that, the high power Tracking and Imaging Radar TIRA at FGAN was cooperating with the highly sensitive receiver of the MPIfR operated 100 m radio telescope Effelsberg in a bi-static configuration.

To enhance the accuracy of the measurements and to provide data for more precise orbit determinations, the development of a cryogenically cooled seven beam receiver for the Effelsberg telescope is ongoing. In parallel to that work, the setup of the digital acquisition and pre-processing back-ends for both, TIRA and the Effelsberg system is in progress.

2. MULTI-USE APPROACH

The application field of the systems involved is not only the measurement of space debris but spans from radio astronomy observations to space reconnaissance tasks.

The Effelsberg radio telescope for instance is used to perform spectroscopic studies to gather information on the physical conditions of objects in the Universe. Multi-feed receivers have enabled very efficient surveys of large areas of sky and significantly improve the signal-to-noise ratio using on-the-fly observing (Stanko et al., 2005). But, up to now the back-ends have not developed at the same pace as the receiver technology. In particular the number of spectral channels and the number of spectrometers could not be increased significantly.

FGAN's radar system TIRA is mainly used for high-precision tracking and high resolution imaging of satellites and aircraft. In the last decades its performance has steadily been increased. But the system still lacks the ability to track unknown objects on a fly-by. Up to now, the system needs a tracking guidance which is provided by the Two Line Element (TLE) data sets of the USSTRATCOM SSN.

For the measurement of space debris, there is still no high power system available in Europe that supports stare and chase. Moreover, the systems still have a large number of analog components with typical problems observed in that domain, e.g. low-frequency interference, thermal drifts, and problems of the reproducibility of settings.

Since the receiver can be identified as the bottleneck in all these systems, a collaboration to utilize synergy effects is strongly suggestive. The goal is to design a system that gives the different parties the power and flexibility for their applications and what's more, let the receiver work in a cost-effective multi-use way.

3. SAMPLING METHODS

As a first step towards a flexible receiver, analog components as shown in Figure 1 have to be replaced by digital ones as far as possible. This results in sampling at the intermediate frequency (IF).

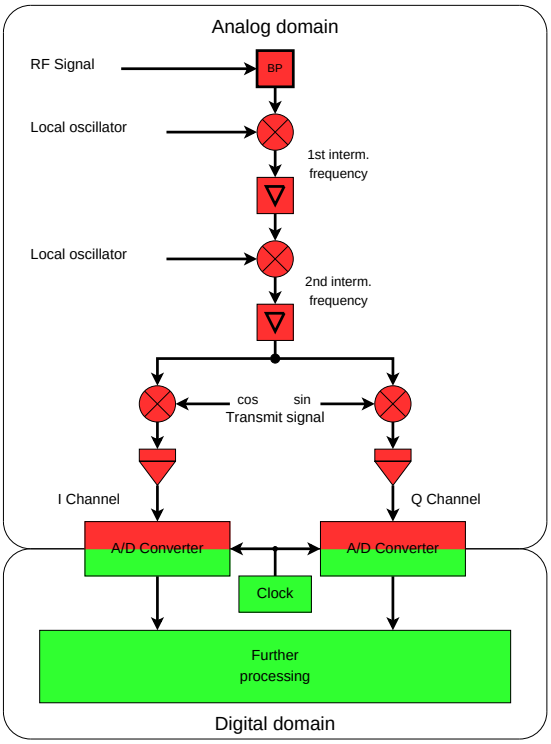

Figure 1. Analog base-band receiver

3.1. Baseband and bandpass sampling

To sample a signal with f_S as its highest frequency component, one has to use a minimum ADC sampling rate $f_{ADC} = 2f_S$. But for band-limited signals it is more convenient to use the deduced version of the sampling theorem originated by Nyquist (1928), Shannon (1948), and Whittaker (1915): Sampling a signal of bandwidth B requires a minimum ADC sampling rate $f_{ADC} = 2B$.

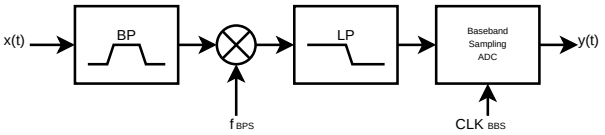

Figure 2. Baseband sampling

Figure 2 illustrates the setup for such a baseband sampling system. First, the band-limited input signal $x(t)$ is mixed down to the baseband by an analog mixer. Afterwards, the resulting signal runs into a low-pass filter and is sampled by an ADC clocked at the baseband sampling frequency f_{BBS}.

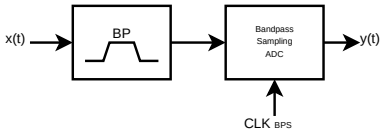

Figure 3. Bandpass sampling

In theory – with ideal components – this setup is identical to that sketched in Figure 3, which now only contains two components: a bandpass filter and an ADC clocked at f_{BPS} with

$$f_{BPS} \gg f_{BBS} \quad . \tag{1}$$

Thus, a bandpass-sampling ADC works like a mixer and a baseband-sampling ADC.

3.2. IF bandpass sampling

In practice bandpass sampling is preferred over baseband sampling since this method

a) reduces the quantization noise,

b) increases the dynamic range,

c) minimizes the parts count,

d) reduces temporal jitter, and

e) eliminates the problem of low-frequency interference and other problems typically observed in the analog/baseband domain.

Besides the elimination of low-frequency interference problems, another substantial feature of bandpass

sampling, especially for the acquisition and processing of weak signals, is the reduction of the quantization noise. Since quantization noise of an ADC is evenly distributed over the entire Nyquist band $0\,Hz \ldots \frac{f_{ADC}}{2}$ and

$$f_{ADC} \gg B_S \tag{2}$$

where f_{ADC} is the ADC sampling frequency and B_S the signal bandwidth, this noise level will be decreased by the process gain PG:

$$PG = 10 \log \left(\frac{f_{ADC}}{2B_S} \right) \quad . \tag{3}$$

From this it follows that the dynamic range of the A/D conversion is increased by keeping the number of the ADC bits.

4. THE NEW RECEIVER LAYOUT

Recent developments in ADC technology can now provide components which are able to work with high sampling rates, and so one can place the ADC close to the signal source and let the receiver sample in the bandpass mode.

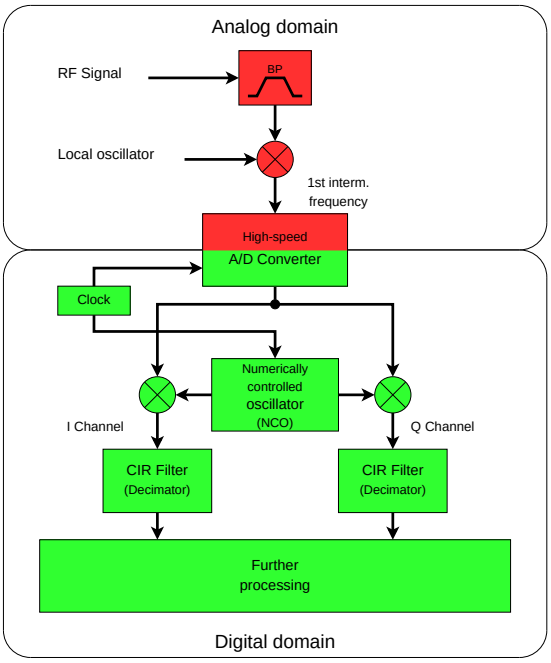

Figure 4. IF-Receiver with digital down conversion

To handle different carrier frequencies and input signal bandwidths efficiently our receiver has two building blocks as shown in Figure 4.

4.1. A/D sampling and down-conversion

After bandpass sampling the incoming signal with a high-speed ADC, a digital mixer quadrature down-converts the signal to the baseband. Since the extraction of the quadrature components I and Q now is done in the digital domain, one will no longer have analog trimming problems.

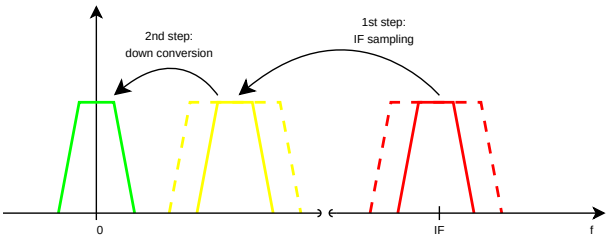

Figure 5. IF-sampling and down-conversion

A digital filter stage then decimates the sampled I and Q channel data by block integration. This results in a reduced data stream which has to be processed subsequent to the acquisition and pre-processing. The maximum allowable decimation is given by the ratio of the signal sampling rate f and the bandwidth B. Figure 5 sketches these band transformations.

Hardware configurations which formerly fixed the systems operational modes can now be modified digitally and enable a short term switch of the system's tasks. Furthermore, with a set of receivers even parallel processing of different tasks is possible.

4.2. FPGA based pre-processing

Pre-processing is no longer concentrated on the software-side and can also be done in hardware, too. The hardware can be reconfigured simply by loading a new image on the field programmable logic gate array (FPGA). Moreover, the FPGA permits high-speed signal pre-processing and data manipulation.

In our applications, we need accurate local time and highly precise relative time information within each of the sampled data streams. To do so, we use a signal provided by the Global Positioning System (GPS) in combination with a high-precision maser time source.

Usually a GPS receiver distributes the time (and position information) by the so called IRIG-B signal which is modulated on a 1 kHz carrier. After a self-calibrating analog comparator, which is used to distinguish between low and high amplitudes, one has to decode the signal. This decoding can be fully done on the FPGA. Here, the time is converted to a BCD coded time stamp using automatic frame identification schemes and a clock recovery technique. This

allows us a precision of 100 μs for the local time and 1 μs for the relative time. Since the IRIG-B decoder module is fully implemented using VHDL, a flexible handling including migration between different FPGA chips is possible.

Thus, high precision time-stamping and other time critical tasks can now be integrated within the data acquisition process. Moreover, the migration of tasks from the CPU to the FPGA reduces the pressure on the operating system.

4.3. Back-end system

The new configuration enables the usage of standard computers to capture the data-stream and to perform additional pre-processing steps. We use Linux as the back-end operating system for two reasons. First, every past and ongoing change is documented and future developments are predictable. This results in low maintenance and development expenses.

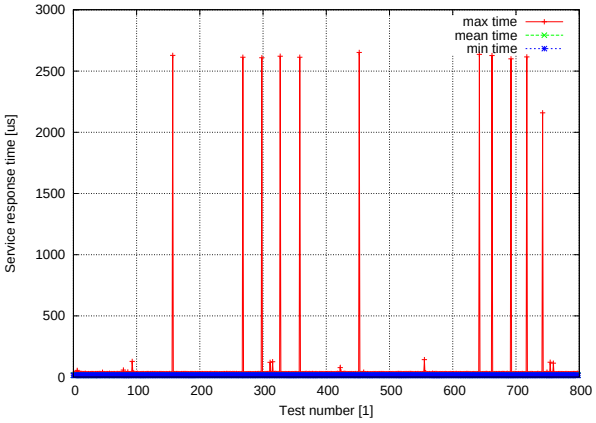

Figure 6. Service Response Times for the 2.4-kernel

Second, we can state that Linux – which is in fact not a real time system – meets all of our real-time requirements. However, this requires an upgrade from the 2.4-kernel to the 2.6-kernel due to the following reasons:

a) The scheduler has a timing which is independent of the number of processes,

b) timer interrupts are generated ten times more often,

c) this kernel supports the preemption even of kernel tasks when there is a task with a higher priority.

Figure 6 and Figure 7 illustrate the service response time (SRT) of our data collection and pre-processing routines on a loaded machine for a representative number of tests. One can notice that the SRT on

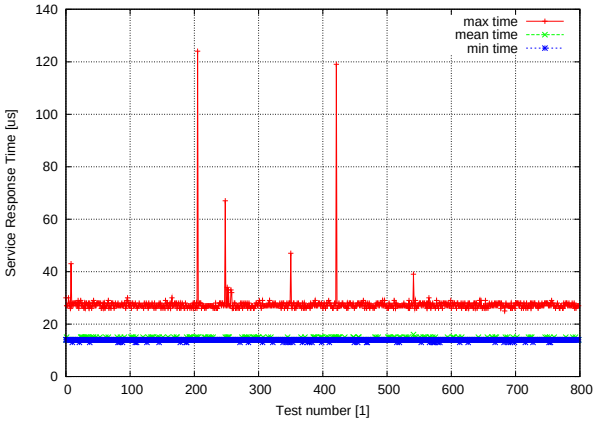

Figure 7. Service Response Times for the 2.6-kernel

system running a 2.4-kernel can reach values up to 2500 μs while the maximum SRT on a 2.6-based system will not exceed 120 μs. This beats our requirements and gives space for future developments.

5. CONCLUSION

For nearly all kinds of space debris, space reconnaissance and astronomy applications the extensive digitalization of the receiver affects the system flexibility. It improves its maintainability, supports a broad range of applications and thus provides the basis to let the system operate in an cost effective multi-use way. Moreover, the digitalization eliminates problems typically observed in the analog domain.

ACKNOWLEDGMENTS

This work was performed under ESA Contract No. 17820/03/D/HK(SC). The authors would like to thank G. Müller (FGAN), I. Krämer (MPIfR) and A. Roy (MPIfR) for their contributions of time to support this work.

REFERENCES

Stanko, S., Klein B., Kerp J.: A Field Programmable Gate Array Spectrometer for Radio Astronomy, Astronomy & Astrophysics accepted, 2005

Nyquist, H.: Certain topics in telegraph transmission theory, AIEE Trans. 47, pp. 617-644, 1928

Shannon, C.E.: A mathematical theory of communications, Bell Syst. Techn. J. 27, pp. 379-423 and pp 623-656, 1948

Whittaker, E.T.: On the functions which are represented by the expansions of the interpolation theory, Proc. R. Soc. Edinburgh 35, pp. 181-194, 1915